

On an analytical optimization of plasma density profiles for downramp injection in laser wake-field acceleration

Gaetano Fiore, Università 'Federico II', and INFN, Napoli, Italy
Paolo Tomassini, IFIN-HH ELI-NP, 077125 Magurele, Romania

AAC24, NIU, Naperville, IL, July 23-27, 2024



Plan

Introduction

Setup & Plane model

1-particle kinematics & some electrodynamics

Collisionless plasma kinematics

Plane collisionless multistream plasma model

Special case: the initial density \tilde{n}_0 is uniform

Hydrodynamic regime up to wave-breaking

Maximizing the WFA of (self-)injected electrons

Motion of a test electron in the plasma wave

Self-injection and maximal WFA by fixing \tilde{n}_0 in 4 steps

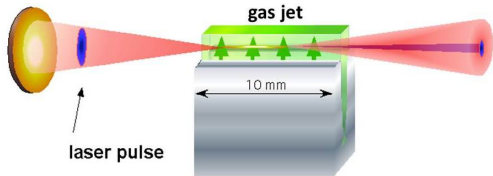
Examples

3D effects, discussion and conclusions

References

Introduction

Laser Wake-Field Acceleration (WFA) [Tajima, Dawson 79] is the first and prototypical mechanism of extreme acceleration of charged particles along short distances: electrons “surf” a plasma wave (PW) driven by a very short laser pulse, e.g. in a supersonic diluted gas jet.



Dynamics is ruled by Maxwell equations coupled to a kinetic theory for plasma electrons, ions. Today these eqs can be solved via more and more powerful PIC codes. However such simulations involve huge costs for each choice of the input data. Therefore it is crucial to run them after a preliminary selection of the input parameters based on a simpler model.

Given a very short & intense plane-wave laser pulse travelling $\parallel \vec{z}$, here we propose a multi-step preliminary analytical procedure to tailor the initial plasma density $\tilde{n}_0(z)$ to the pulse, so as to control:

1. the formation of the plasma wave (PW);
2. its wave-breaking (WB) at density inhomogeneities; ;
3. the self-injection of low-charge bunches of plasma electrons in the PW by the first WB at the density down-ramp;
4. to maximize the initial stages of the LWFA of the latter.

To this end, we *invert* our resolution procedure of the following *direct problem* : given $\tilde{n}_0(z)$ and laser pulse, determine the motion of the plasma electrons. Such a resolution is based on a multi-stream, fully relativistic plane model, which is valid as long as the pulse depletion can be neglected.

To make the *inversion formulae* manageable, we stick to slowly varying $\tilde{n}_0(z)$.

We check the effectiveness of the \tilde{n}_0 resulting from the inversion formulae, and can then further improve it by fine-tuning, solving again the direct problem numerically (first the eqs of our plane model, then applying PIC codes).

Finally, we determine the detailed density and energy distribution of the WFA electrons by FB-PIC simulations.

Setup & Plane model

Input = nontrivial initial data:

- a) the function $\tilde{n}_0(z) \geq 0$, with $\tilde{n}_0(z)=0$ if $z < 0$, $\tilde{n}_0(z) \leq n_B < \infty$ if $z > 0$, yielding the initial electron and proton densities n_e, n_p :

$$\mathbf{v}_e(0, \mathbf{x}) = \mathbf{0}, \quad n_e(0, \mathbf{x}) = n_p(0, \mathbf{x}) = \tilde{n}_0(z); \quad (1)$$

- b) the vector-valued function $\epsilon^\perp(\xi)$ yielding the initial laser-pulse EM fields:

$$\mathbf{E}(t, \mathbf{x}) = \epsilon^\perp(ct - z), \quad \mathbf{B} = \mathbf{B}^\perp = \mathbf{k} \times \mathbf{E}^\perp \quad \text{if } t \leq 0, \quad (2)$$

support(ϵ^\perp) $\subseteq [0, l]$ with $l \lesssim \sqrt{\pi mc^2 / n_B e^2}$: the pulse reaches the plasma at $t=0$ & overshoots all e^- before their z reach the 1st minimum < 0 (ES pulse).

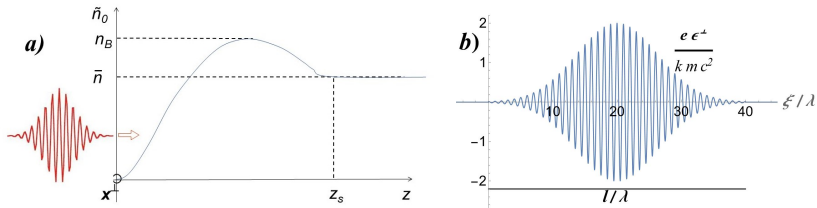
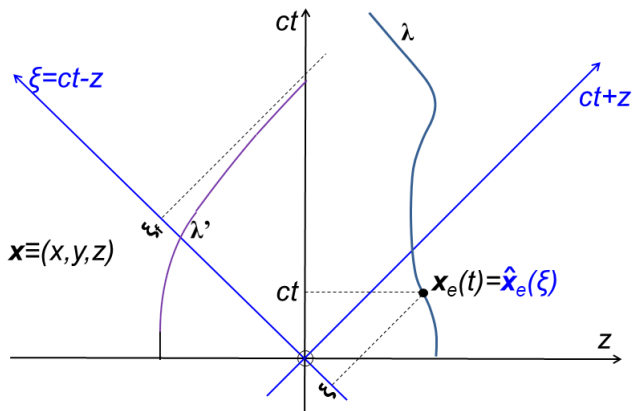


Figure 1: Here: $\tilde{n}_0(z)$ has down-ramp + plateau \bar{n} as a); ES, SMM pulse as b)

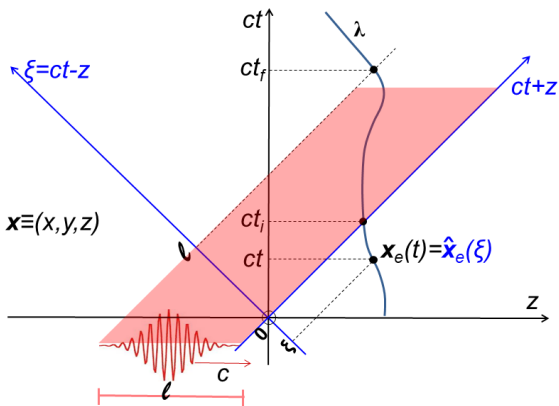
1-particle kinematics & some electrodynamics



As every particle travels slower than light, $\tilde{\xi}(t) = ct - z(t)$ grows strictly, and $\xi = ct - z$ can replace t as the independent parameter along its worldline (WL) λ (in Minkowski space) and in its equation of motion (EoM). Clock=pulse.

WL λ' : $v^z \rightarrow c$ as $t \rightarrow \infty \Leftrightarrow \xi \rightarrow \xi_f < \infty$.

We will use: CGS units; dimensionless $\beta \equiv \dot{\mathbf{x}}/c$, $\gamma \equiv 1/\sqrt{1-\beta^2}$, 4-velocity $u = (u^0, \mathbf{u}) \equiv (\gamma, \gamma\boldsymbol{\beta}) = \left(\frac{p^0}{mc^2}, \frac{\mathbf{p}}{mc}\right)$, $s \equiv \gamma - u^z > 0$. $s \rightarrow 0$ implies $u^z \rightarrow \infty$.



How to simplify the Lorentz EOM

$$\dot{\mathbf{p}}(t) = q \epsilon^\perp [ct - z(t)] + \mathbf{k} q E^z(t, z) + (q/c) \mathbf{v}(t) \times \{ \mathbf{k} \times \epsilon^\perp [ct - z(t)] \} \quad ? \quad (3)$$

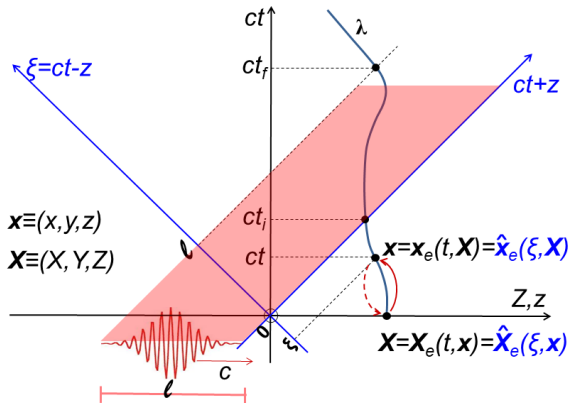
Changing variables $t \mapsto \xi$, $p^z \mapsto p^- \equiv p^0/c - p^z = mc s$ transforms (3) into

$$\hat{\mathbf{p}}^{\perp'}(\xi) = q \epsilon^\perp(\xi)/c, \quad \hat{s}'(\xi) = \frac{-q}{mc^2} \check{E}^z(\xi, \hat{z}) \quad (4)$$

($\epsilon^\perp \not\propto$ unknown $z(t)$). If $E^z = 0$ and $\mathbf{p}(0) = 0$ these are immediately solved by $s = 1$, $\hat{\mathbf{p}}^\perp(\xi) = (q/c) \int_{-\infty}^{\xi} d\zeta \epsilon^\perp(\zeta) =: (-q/c) \alpha^\perp(\xi)$, $\Rightarrow p^z = \mathbf{p}^{\perp 2} / 2mc$.

Collisionless plasma kinematics

We regard ions as immobile. No collisions \Rightarrow : all e^- having the same position \mathbf{X} and velocity \mathbf{V} at $t = 0$ will have the same position $\mathbf{x}_e(t, \mathbf{X}, \mathbf{V})$ and velocity $\dot{\mathbf{x}}_e(t, \mathbf{X}, \mathbf{V})$ at $t > 0$. Since here $\mathbf{V} = \mathbf{0}$ for all e^- , then $\mathbf{x}_e = \mathbf{x}_e(t, \mathbf{X})$. The *hydrodynamic regime* (HR) lasts as long as $\mathbf{X} \mapsto \mathbf{x}$ are 1-to-1, i.e. WLs do not intersect. Afterwards: *multistream* or *post-hydrodynamic regime* (PHR).



HR: Eulerian observable $f(t, \mathbf{x}) = \check{f}(\xi, \mathbf{x}) = \tilde{f}(t, \mathbf{X}) = \hat{f}(\xi, \mathbf{X})$ Lagrangian obs.

Plane collisionless multistream plasma model

Transverse plane symmetry implies:

Eulerian fields can depend only on t, z ;

their Lagrangian counterparts and the displacements

$\Delta_e \equiv \mathbf{x}_e(t, \mathbf{X}) - \mathbf{X}$ can depend only on t, Z ;

their “hatted” Eulerian/Lagrangian counterparts can depend only on ξ, z , resp. ξ, Z .

The rigid motion of each electrons' transverse sheet (=very thin layer) is codified by $z_e(t, Z)$ [or $\hat{z}_e(\xi, Z)$].

Different sheets may cross each other (see e.g. [Dawson62]); the HR lasts as long as this does not occur.



Maxwell equations $\nabla \cdot \mathbf{E} = 4\pi j^0$, $\frac{1}{c} \partial_t E^z + 4\pi j^z = (\nabla \wedge \mathbf{B})^z = 0$ are solved by

$$E^z(t, z) = 4\pi e [\tilde{N}(z) - N_e(t, z)], \quad (5)$$

$$\tilde{N}(z) \equiv \int_0^z d\zeta \tilde{n}_0(\zeta), \quad N_e(t, z) \equiv \int_0^\infty dZ \tilde{n}_0(Z) \theta[z - z_e(t, Z)]. \quad (6)$$

[GF,PT24] $\tilde{N}(z)$, $N_e(t, z)$ resp. are the #(protons), #(electrons) per unit transverse surface with $z' \leq z$ at time t .

Simplest gauge choice: also $A = (A^0, \mathbf{A})$ depends only on t, z , and

$$\mathbf{A}^\perp(t, z) \equiv -c \int_{-\infty}^t dt' \mathbf{E}^\perp(t', z) \quad (\text{physical observable}); \quad (7)$$

Since $\mathbf{u}_e^\perp(0, \mathbf{x}) = \mathbf{0}$, Lorentz eq. implies $\mathbf{u}_e^\perp = e\mathbf{A}^\perp/mc^2$.

$$\text{For } t \leq 0 \quad \mathbf{A}^\perp(t, z) = \boldsymbol{\alpha}^\perp(ct-z), \quad \boldsymbol{\alpha}^\perp(\xi) \equiv -\int_{-\infty}^{\xi} d\zeta \boldsymbol{\epsilon}^\perp(\zeta). \quad (8)$$

We can reformulate Maxwell eq. $\square \mathbf{A}^\perp = 4\pi \mathbf{j}^\perp$ as the integral eq.

$$\mathbf{A}^\perp(t, z) - \boldsymbol{\alpha}^\perp(ct-z) = -\frac{K}{2} \int d\eta d\zeta \theta(\eta) \theta(ct-\eta-|z-\zeta|) \left(\frac{n_e \mathbf{A}^\perp}{\gamma_e} \right)(\eta, \zeta), \quad (9)$$

$K \equiv \frac{4\pi e^2}{mc^2}$. Neglecting pulse depletion, $\mathbf{A}^\perp(t, z) = \boldsymbol{\alpha}^\perp(ct-z)$. The remaining eqs to solve is the family (parametrized by Z) of ordinary Cauchy problems

$$\hat{z}'_e(\xi, Z) = \frac{1+v(\xi)}{2\hat{s}^2(\xi, Z)} - \frac{1}{2}, \quad (10)$$

$$\hat{s}'(\xi, Z) = \frac{e\check{E}^z}{mc^2} = K \left\{ \tilde{N}[\hat{z}_e(\xi, Z)] - \int_0^\infty d\zeta \tilde{n}_0(\zeta) \theta[\hat{z}_e(\xi, Z) - \hat{z}_e(\xi, \zeta)] \right\}, \quad (11)$$

$$\hat{z}_e(0, Z) = Z, \quad \hat{s}(0, Z) = 1, \quad (12)$$

in the unknowns $\hat{s}(\xi, Z)$, $\hat{z}_e(\xi, Z)$. Here $v(\xi) \equiv (e\boldsymbol{\alpha}^\perp(\xi)/mc^2)^2$.

HR: dynamics reduced to decoupled Hamiltonian ODEs for 1-dim systems

As long as the HR holds, eqs (10-12) for different Z 's *decouple* and become eqs

$$\hat{\Delta}' = \frac{1+v}{2\hat{s}^2} - \frac{1}{2}, \quad \hat{s}' = K \left\{ \tilde{N}[Z+\hat{\Delta}] - \tilde{N}(Z) \right\}, \quad (13)$$

$$\hat{\Delta}(0, Z) = 0, \quad \hat{s}(0, Z) = 1 \quad (14)$$

[GF18] in the unknowns $\hat{\Delta}(\xi, Z) \equiv \hat{z}_e(\xi, Z) - Z$, $\hat{s}(\xi, Z)$, $\hat{\xi}(\xi, Z)$. For each $Z \geq 0$ (13) are **Hamilton equations** $q' = \partial \hat{H} / \partial p$, $p' = -\partial \hat{H} / \partial q$ of a **1-dim system**: $\xi, \hat{\Delta}, -\hat{s}$ play the role of t, q, p , and the Hamiltonian up to mc^2 reads

$$\begin{aligned} \hat{H}(\hat{\Delta}, \hat{s}, \xi; Z) &:= \frac{\hat{s}^2 + 1 + v(\xi)}{2\hat{s}} + \mathcal{U}(\hat{\Delta}; Z), \\ \mathcal{U}(\Delta; Z) &:= K \int_0^\Delta d\zeta (\Delta - \zeta) \tilde{n}_0(Z + \zeta). \end{aligned} \quad (15)$$

For $\xi > l$ $v = \text{const}$, $\hat{H} = h(Z) = \text{const}$, (13) are autonomous and **can be solved by quadrature**; if $Z > 0$ the solutions are periodic in ξ ; $\xi_H(Z) \equiv \text{period}$.

All other unknowns can be expressed via $(\hat{\Delta}, \hat{s})$:

$$\hat{\mathbf{u}}^\perp = \frac{e \alpha^\perp(\xi)}{mc^2}, \quad \hat{u}^z = \frac{1 + \hat{\mathbf{u}}^{\perp 2} - \hat{s}^2}{2\hat{s}}, \quad \hat{\gamma} = \frac{1 + \hat{\mathbf{u}}^{\perp 2} + \hat{s}^2}{2\hat{s}}, \quad (16)$$

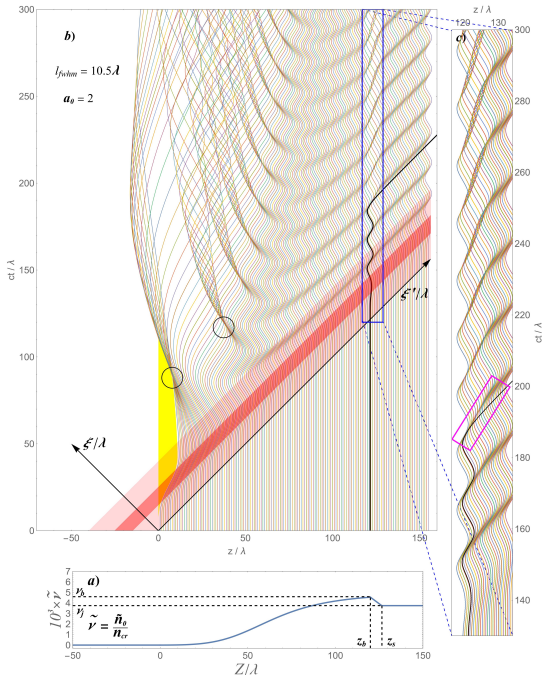
$$\hat{\mathbf{x}}_e^\perp(\xi, \mathbf{X}) - \mathbf{X}^\perp = \int_0^\xi d\eta \frac{\hat{\mathbf{u}}^\perp(\eta)}{\hat{s}(\eta, Z)}, \quad \hat{z}_e(\xi, \mathbf{X}) - Z = \hat{\Delta}(\xi, Z). \quad (17)$$

a) “Optimal” $\tilde{n}_0(z)$ for the above pulse: $\bar{n} = \bar{n}^j = n_{cr}/268$, $n_b = 1.28 \times \bar{n}^j$, $z_B = 120\lambda$, $z_s - z_B = 6.6\lambda$ [GF 2023].

b) WLs of e^- with $Z = 0, \lambda, \dots, 156\lambda$ are obtained solving (13-14) and look as plot until they first intersect (circles), \Rightarrow WBs. The black WL of the e^- self-injected by the earliest WB holds **for all** t ; after WB it is ruled by (22).

The yellow region is filled only by ions; in the pink region ($0 < \xi < 40\lambda$) the pulse modulating intensity ϵ_s^2 is nonzero; in the red region ($|\xi - 20\lambda| < 5.25\lambda$) ϵ_s^2 is above half maximum.

c) Zoom of the blue box in a).



Hydrodynamic regime up to wave-breaking

The HR holds as long as $\hat{J} \equiv \left| \frac{\partial \hat{x}_e}{\partial X} \right| = \frac{\partial \hat{z}_e}{\partial Z} > 0$. For $\xi > l$ [GF et al 23]

$$\hat{J}(\xi + k\xi_H, Z) = \hat{J}(\xi, Z) - k \frac{\partial \xi_H}{\partial Z} \Delta'(\xi, Z), \quad \forall k \in \mathbb{N}, Z \geq 0, \quad (19)$$

$$\Leftrightarrow \hat{J}(\xi, Z) = a(\xi, Z) + \xi b(\xi, Z), \quad (20)$$

where $b \equiv -\frac{\partial \log \xi_H}{\partial Z} \hat{\Delta}'$, $a \equiv \hat{J} - \xi b$ are ξ_H -periodic in ξ , and b has zero mean over a period (apply ∂_Z to $\Delta[\xi + n\xi_H(Z), Z] = \Delta(\xi, Z)$, use ξ_H -periodicity of Δ').

By (19) we can extend our knowledge of \hat{J} from $[l, l + \xi_H[$ to all $\xi \geq l$.

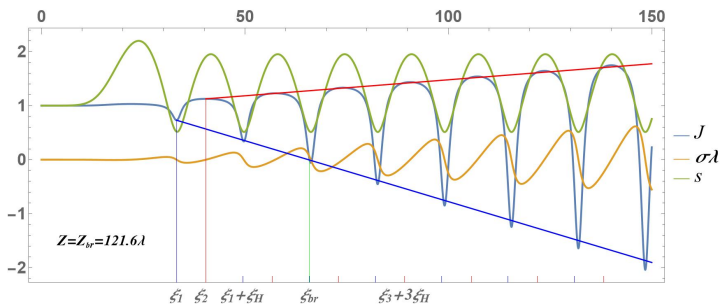


Figure 4: $\hat{J}, \hat{\sigma}$ vs. ξ for $Z = Z_b \simeq 121.6\lambda$ and input data as in Fig. 3.

Maximizing the WFA of (self-)injected e^-

Motion of test electrons in the plasma wave

The eqs for a *test* e^- sheet injected in the PW behind the pulse reduce to

$$\hat{z}'_i = \frac{1 - \hat{s}_i^2}{2\hat{s}_i^2}, \quad \hat{s}'_i = M\Delta \quad (22)$$

along the density plateau, and $\hat{s}_i(\xi) - s(\xi) = \delta s \equiv s_{i0} - s(\xi_0) = \text{const}$, cf (18b).
If $\delta s < -s_m$ (**trapping condition**), then $\exists \xi_f > \xi_0$ s.t. $\hat{s}_i(\xi_f) = 0$, e^- is **trapped & accelerated in a trough of the PW**. As $t \rightarrow \infty$

$$z_i \sim ct, \quad \gamma_i \simeq F z_i / \lambda \xrightarrow{z_i \rightarrow \infty} \infty, \quad (23)$$

$F \equiv K \bar{n} \lambda |\Delta(\xi_f)|$; reliable as long as pulse depletion is negligible: $z_i \leq z_{pd}$.

Fixed \bar{n} , if $\delta s = -1$, then $|\Delta(\xi_f)| = |\Delta_m| = \Delta_M$, and F is maximal:

$$\gamma_i(z_i; \bar{n}) \simeq \sqrt{j(\bar{n})} z_i / \lambda; \quad (24)$$

here $j(\bar{n}) \equiv \bar{n} [\bar{h}(\bar{n}) - 1] 8\pi^2 / n_{cr}$, $\bar{h}(\bar{n}) =$ final energy transferred by the pulse to the plateau plasma electrons. Physically, $|\Delta(\xi_f)| = \Delta_M$ means that the test sheet tends to the transverse plane of the travelling bucket where $|E^z|$ is maximal. Below $\nu \equiv n_0 / n_{cr}$.

Self-injection & maximal WFA by fixing \tilde{n}_0 in 4 steps

Step 1: Computing $\bar{h}(\nu), j(\nu)$.

(We interpolate 200 points; few seconds via *Mathematica*).

Step 2: Optimal plateau density \bar{n} .

If the depth available for WFA is $z_i \leq z_{pd}(\nu_j)$, set $\bar{n}/n_{cr} = \nu_j \equiv \max\{j(\nu)\}$:

$$\gamma_i^M(z_i) \simeq \sqrt{j(\nu_j)} z_i / \lambda. \quad (25)$$

Step 3: \tilde{n}_0 with optimal down-ramp for self-injection, LWFA.

$$\tilde{n}_0(Z) = \bar{n} + \Upsilon(Z - z_s), \quad z_B \leq Z \leq z_s,$$

$\Upsilon = \frac{\bar{n} - n_B}{z_s - z_B}$. Let (ξ_b, Z_b) be the pair (ξ, Z) with smallest ξ s.t. $\hat{J}(\xi, Z) = 0$. The $Z_b e^-$ are the fastest injected & trapped in a PW trough by the 1st WB. We fix Υ, z_B requiring: $\delta s = -1$, so that (24) applies; no WBDLPI.

Step 4: Choosing an up-ramp of \tilde{n}_0

out of the ∞ -ly many ones growing from 0 to n_B and preventing WB for $\xi < \xi_b$; $\tilde{n}_0(z) \simeq O(z^2)$ [GF et al 2022-23].

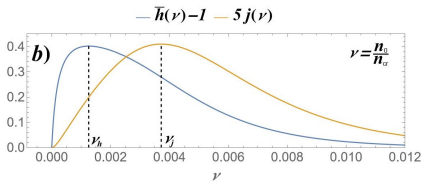


Figure 5: $\bar{h}-1$ (energygain per plasma e^-) and j by the pulse of fig. 2a, vs. ν

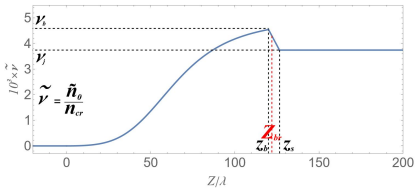


Figure 6: Optimal density associated to the pulse of fig. 2a, used in fig. 3.

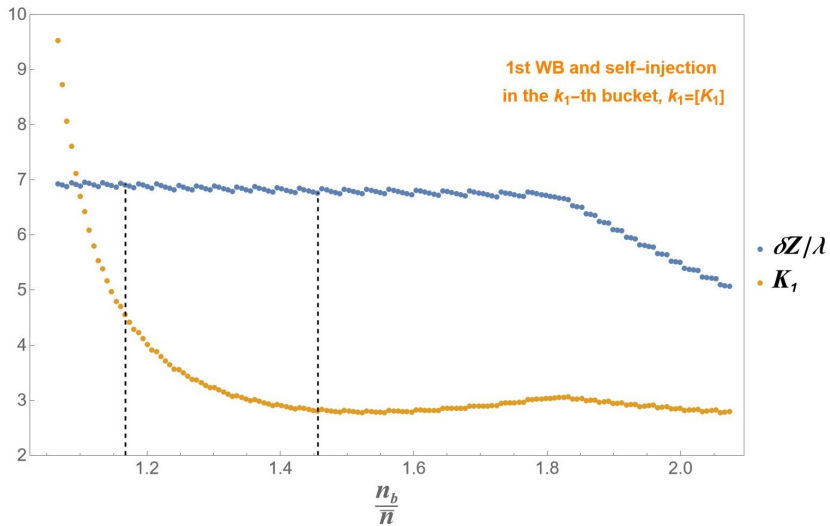


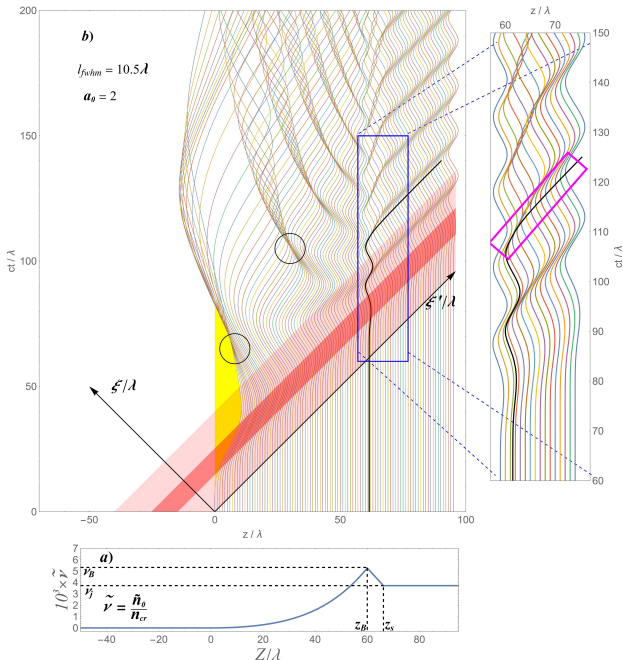
Figure 7

Examples

a) Another “optimal” $\tilde{n}_0(z)$ for the above pulse: $\bar{n} = \bar{n}^j = n_{cr}/268$,
 $n_b = 1.32 \times \bar{n}^j$,
 $n_B = 1.42 \times \bar{n}^j$,
 $z_B = 60\lambda$, $z_s - z_B = 6.2\lambda$.

b) WLs of e^- with $Z = 0, \lambda, \dots, 95\lambda$ as plot are Ok until they first intersect (circles), \Rightarrow WBs. The black WL of the e^- self-injected by the earliest WB is Ok **for all t** . Nearly maximal $F = 0.286$. If $\lambda = 0.8\mu\text{m}$, this leads to a remarkable energy gain of 0.182MeV per μm .

c) Zoom of blue box.



Choosing the input data of fig.s 3, 8, we resp. find **SLIDESHOWS**

3D effects, discussion and conclusions

Summarizing, the steps of our preliminary optimization process are:

1. finding the final energy \bar{h} transferred by the pulse to the plateau plasma electrons and $j = 8\pi^2 [\bar{h}-1] \bar{n}/n_{cr}$ as functions of the density \bar{n} ;
2. finding the 'optimal' value \bar{n}^j of \bar{n} maximizing $j(\bar{n})$;
3. finding the 'optimal' length $z_B - z_s$ and slope Υ of the density down-ramp;
4. adjusting the up-ramp ($z < z_B$) of $\tilde{n}_0(z)$ to avoid WB for $\xi < \xi_b$.

Range of applicability of the model?

The depletion of the pulse is negligible in the tilted (rather long) rectangle

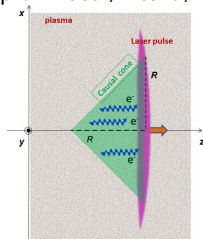
$$0 \leq ct - z \leq l, \quad 0 \leq ct + z \lesssim mc^2/e^2 \bar{n} \lambda \quad (26)$$

Pulse cylindrically symmetric around \vec{z} with waist R : by causality our results hold strictly in the green causal cone trailing the pulse, approximately nearby.

In particular, if the pulse has maximum at $\xi = \frac{l}{2}$, and

$$R > \xi_b - \frac{l}{2}, \quad R \gg \frac{a_0 \lambda}{2\pi} \left[\bar{h} + \sqrt{\bar{h}^2 - 1} \right] \quad (27)$$

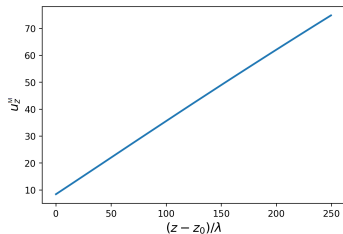
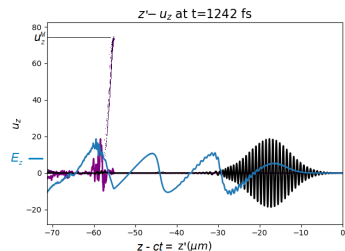
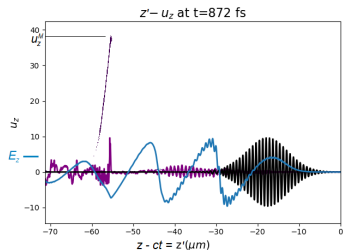
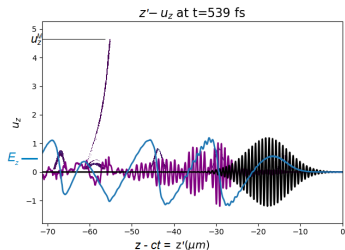
then the $\mathbf{X} \simeq (0,0,Z_b) e^-$ keep in that cone and move as above: same maximal WFA, as far as pulse not depleted.













Apply our optimization procedure to the pulse of Fig. 2a ($a_0 = 2$, $I_{fwhm} = 10\lambda$): we find the initial density $\tilde{n}_0(z)$ and the WLs of Fig. 3; $F = 0.28$.

Ti-sapphire laser: $\lambda \simeq 0.8\mu\text{m}$; 'moderate' peak intensity $\mathcal{I} = 1.7 \times 10^{19} \text{W/cm}^2$ yields the remarkable energy gain 1.8 GeV/cm of the Z_b electron (black WL).

Good agreement with 2D FB-PIC simulations (courtesy of P. Tomassini):



References

-  G. Fiore, P. Tomassini, *On plasma densities maximizing laser wake field acceleration*, forthcoming paper.
-  G. Fiore, *A preliminary analysis for efficient laser wakefield acceleration*, arXiv:2305.04580. To appear in the Proceedings of the 20th Advanced Accelerator Concepts Workshop (AAC22), November 6-11, 2022.
-  G. Fiore, T. Akhter, S. De Nicola, R. Fedele, D. Jovanović, Phys. D: Nonlinear Phenom., **454** (2023), 133878.
-  G. Fiore, M. De Angelis, R. Fedele, G. Guerriero, D. Jovanović, Mathematics **10** (2022), 2622; Ricerche Mat. (2023).
-  G. Fiore, P. Catelan, Nucl. Instr. Meth. Phys. Res. **A909** (2018), 41-45.
-  G. Fiore, J. Phys. A: Math. Theor. **51** (2018), 085203.
-  G. Fiore, J. Phys. A: Math. Theor. **47** (2014), 225501.
-  G. Fiore, R. Fedele, U. de Angelis, Phys. Plasmas **21** (2014), 113105.
-  G. Fiore, S. De Nicola, Phys. Rev. Acc. Beams **19** (2016), 071302 (15pp).
-  G. Fiore, Ricerche Mat. **65** (2016), 491-503.